DRUGS

Airway relaxation mechanisms and structural basis of osthole for improving lung function in asthma

Sheng Wang[1,2,3]*, Yan Xie[2]*, Yan-Wu Huo[1], Yan Li[4], Peter W. Abel[2], Haihong Jiang[2], Xiaohan Zou[4], Hai-Zhan Jiao[1,3], Xiaolin Kuang[1,3], Dennis W. Wolff[5], You-Guo Huang[1], Thomas B. Casale[6], Reynold A. Panettieri Jr.[7], Taotao Wei[1†], Zhengyu Cao[4†], Yaping Tu[2†]

Overuse of β2-adrenoceptor agonist bronchodilators evokes receptor desensitization, decreased efficacy, and an increased risk of death in asthma patients. Bronchodilators that do not target β2-adrenoceptors represent a critical unmet need for asthma management. Here, we characterize the utility of osthole, a coumarin derived from a traditional Chinese medicine, in preclinical models of asthma. In mouse precision-cut lung slices, osthole relaxed preconstricted airways, irrespective of β2-adrenoceptor desensitization. Osthole administered in murine asthma models attenuated airway hyperresponsiveness, a hallmark of asthma. Osthole inhibited phosphodiesterase 4D (PDE4D) activity to amplify autocrine prostaglandin E$_2$ signaling in airway smooth muscle cells that eventually triggered cAMP/PKA-dependent relaxation of airways. The crystal structure of the PDE4D complexed with osthole revealed that osthole bound to the catalytic site to prevent cAMP binding and hydrolysis. Together, our studies elucidate a specific molecular target and mechanism by which osthole induces airway relaxation. Identification of osthole binding sites on PDE4D will guide further development of bronchodilators that are not subject to tachyphylaxis and would thus avoid β2-adrenoceptor agonist resistance.

INTRODUCTION

Asthma, a chronic inflammatory disease, is characterized physiologically by airway flow obstruction and airway hyperresponsiveness (AHR). Clinically, asthma with intermittent symptoms is treated with β2-adrenoceptor agonists such as albuterol (*1*), whereas inhalation of corticosteroids such as fluticasone is the first choice for the treatment of asthma and airway inflammation. A combination of corticosteroid and long-acting β2-adrenoceptor agonists (LABAs) such as salmeterol or formoterol is often used when corticosteroid monotherapy becomes inadequate (*2*). However, overuse of β2-adrenoceptor agonists induces β2-adrenoceptor desensitization that decreases bronchodilator efficacy (*3*), thus necessitating the identification of new agents to reverse unresponsive airway constriction.

Activation of β2-adrenoceptors by its agonists increases adenosine 3′,5′-monophosphate (cAMP) levels in airway smooth muscle (ASM) cells to promote bronchodilation (*1*). Prostaglandin E$_2$ (PGE2), an abundant prostanoid in the body (*4*), also functions as an endogenous bronchodilator. PGE2 can bind to four cell surface G protein–coupled prostanoid receptors termed EP1 to EP4 (*5*). Similar to β2-adrenoceptors, EP2 and EP4 are coupled through G$_s$ proteins to adenylyl cyclase, which converts adenosine 5′-triphosphate to cAMP. Increased cAMP activates protein kinase A (PKA) to phosphorylate

various target proteins to induce ASM relaxation (*6*). The intracellular cAMP level is determined by adenylyl cyclase–dependent generation and phosphodiesterase (PDE)–dependent degradation. There are at least 11 PDE families of 24 genes. Different cell types express unique PDE isoforms to achieve spatial control of intracellular cAMP signaling (*7*). Several subfamilies of PDE are expressed in human ASM cells, with PDE3 and PDE4 being primarily responsible for cAMP hydrolysis (*8, 9*). The PDE4 subfamily contains four genes coding the subtypes PDE4A/B/C/D, and PDE4D is the predominant isoform that controls airway constriction (*10, 11*). Roflumilast, a U.S. Food and Drug Administration–approved orally active PDE4 inhibitor for treating severe chronic obstructive pulmonary disease, shows bronchodilator activity and has been studied for asthma.

Osthole is a bioactive natural coumarin derived from the plant *Cnidium monnieri* (She Chuang Zi), a widely used traditional Chinese medicine for treating impotence and skin diseases (*12*). Pharmacological investigations have revealed various bioactivities of osthole including neuroprotection, anti-oxidation, anti-inflammation, and cardiovascular protective effects (*13*). Osthole displays anti-asthmatic activity in an ovalbumin-induced murine asthma model (*14, 15*). It inhibits the activation of nuclear factor κB (*14*) and cyclooxygenase-2 (COX-2) (*16*), which likely explains the anti-inflammatory properties of osthole in allergic asthma inflammation. Dendritic cells and T cells have been suggested to be the target cells responsible for the ability of osthole to ameliorate allergic asthma (*15*). Osthole also relaxes rat thoracic aorta and guinea pig tracheal muscle (*17–19*), suggesting that it may exhibit bronchodilation effects. However, the bronchodilator pathways and processes activated by osthole and its molecular mechanisms of action remain elusive.

In the present study, we found that osthole relaxed β2-adrenoceptor–desensitized small airways of mouse lung slices ex vivo and ameliorated AHR in murine models of asthma. Further mechanistic studies and structural analysis revealed that osthole functioned as a PDE4D inhibitor to amplify autocrine PGE2 signaling through G$_s$ protein–coupled

[1]National Laboratory of Biomacromolecules, Institute of Biophysics, Chinese Academy of Sciences, Beijing 100101, China. [2]Department of Pharmacology and Neuroscience, Creighton University School of Medicine, Omaha, NE 68178, USA. [3]University of Chinese Academy of Sciences, Beijing 100049, China. [4]State Key Laboratory of Natural Medicines and Jiangsu Provincial Key Laboratory for TCM Evaluation and Translational Development, China Pharmaceutical University, Nanjing 211198, China. [5]Kansas City University of Medicine and Biosciences-Joplin, Joplin, MO 64804, USA. [6]Department of Internal Medicine, University of South Florida School of Medicine, Tampa, FL 33612, USA. [7]Rutgers Institute for Translational Medicine and Science, Rutgers Biomedical and Health Sciences, Rutgers University, New Brunswick, NJ 08901, USA.
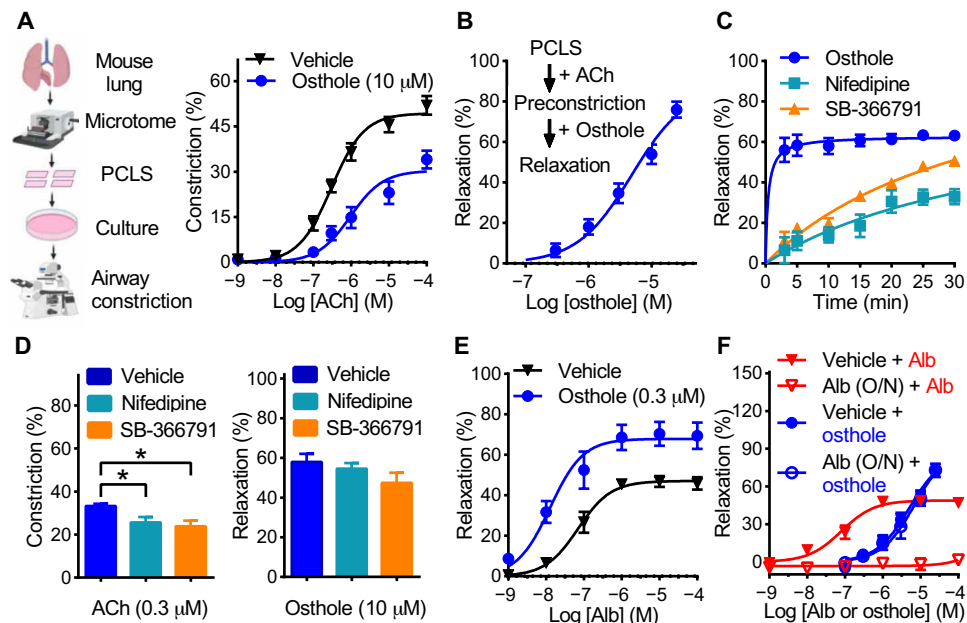*These authors contributed equally to this work.
†Corresponding author. Email: yat60399@creighton.edu (Y.T.); weitt@moon.ibp.ac.cn (T.W.); zycao1999@hotmail.com (Z.C.)

receptors EP2 and EP4 in ASM cells, which then caused cAMP/PKA-dependent relaxation of constricted airways that were unresponsive to β2-adrenoceptor agonists. Thus, osthole may represent a promising therapeutic agent for the treatment of asthmatic patients with airway constriction and hyperresponsiveness despite LABA and inhaled corticosteroid use.

RESULTS

Osthole induces relaxation of small airways in mouse precision-cut lung slices ex vivo

The muscarinic receptor agonist acetylcholine (ACh) induced a concentration-dependent airway constriction in mouse precision-cut lung slices (PCLS) with a median effective concentration (EC$_{50}$) value of 301 ± 41 nM and a maximal constriction (E_{max}) of 49.3 ± 1.4% (Fig. 1A). Pretreatment of PCLS with 10 μM osthole reduced ACh-induced airway constriction by decreasing the E_{max} to 30.3 ± 1.8% and increasing the EC$_{50}$ of ACh to 957 ± 263 nM. We also preconstricted airways of mouse PCLS with ACh to produce a rapid and persistent submaximal airway constriction of 32.0 ± 6.0%. Repeated addition of osthole induced a concentration-dependent relaxation of preconstricted airways to near 80% at 25 μM with an EC$_{50}$ of 4.8 ± 1.3 μM (Fig. 1B).

L-type Ca$_v$1.2 and TRPV1 channels are not involved in osthole-induced airway relaxation

Osthole can block L-type Ca$_v$1.2 calcium channels and directly inhibit TRPV1 (transient receptor potential cation channel subfamily V1) activity (20, 21). We compared airway relaxation dynamics induced by 10 μM osthole, the Ca$_v$1.2 channel blocker nifedipine, or the TRPV1 antagonist SB-366791. Osthole induced a rapid airway relaxation of 60% within 5 min that was sustained for 30 min. In contrast, nifedipine or SB-366791 caused a very slow relaxation that did not reach maximal relaxation until 25 min after treatment (Fig. 1C). Furthermore, although pretreatment with nifedipine or SB-366791 reduced ACh-induced airway constriction by about 25%, they did not affect osthole-induced relaxation of ACh-preconstricted airways in a statistically significant manner (Fig. 1D).

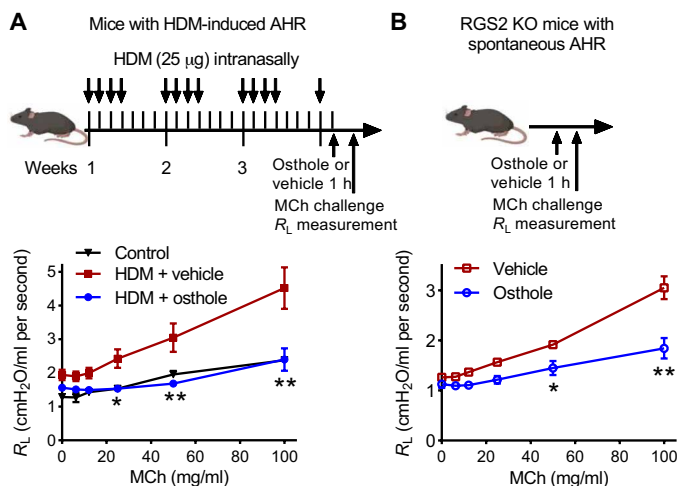### Osthole potentiates albuterol-induced airway relaxation

The β2-adrenoceptor agonist albuterol is widely used as a bronchodilator to treat asthma. Pretreatment with 0.3 μM osthole alone induced less than 10% relaxation of preconstricted mouse airways but caused a sixfold leftward shift in the concentration response curve for albuterol-induced relaxation, and the E_{max} of albuterol was increased from 47.1 ± 1.6 to 67.9 ± 3.3% (Fig. 1E). Thus, pretreatment with osthole increases both apparent potency and efficacy of albuterol.

Osthole relaxes β2-adrenoceptor desensitized airways

To desensitize β2-adrenoceptors, mouse PCLSs were treated with albuterol (100 μM) overnight before being washed and exposed to increasing concentrations of albuterol. Baseline airway tone was only slightly increased, but the relaxation response was attenuated (Fig. 1F), suggesting that overnight treatment with albuterol caused desensitization of β2-adrenoceptors in airways. However, osthole-dependent relaxation of airways was still maintained with similar efficacy and potency irrespective of β2-adrenoceptor desensitization (EC$_{50}$ of 7.0 ± 2.5 μM control compared to 5.0 ± 1.3 μM desensitization) (Fig. 1F). This result indicates that the relaxation effect of osthole persisted after β2-adrenoceptors were desensitized.

Osthole ameliorates AHR in mice

We next investigated whether osthole ameliorates AHR in murine models of asthma. Three weeks of intranasal exposure to house dust mite (HDM), the most prevalent allergen associated with asthma, caused a decline in lung function as indicated by elevated lung resistance and resulted in AHR to inhaled methacholine (MCh) compared to naïve mice (Fig. 2A). A single oral dose of osthole (2.5 mg/10 g of body weight) blocked the increase in lung resistance to MCh in HDM-treated mice such that

Fig. 1. Osthole elicits a fast and prolonged relaxation of small airways in mouse PCLS, enhances albuterol-induced relaxation, and maintains its potency and efficacy after β2-adrenoceptor desensitization. (**A**) Concentration-response curves for acetylcholine (ACh)–induced constriction of airways pretreated with 10 μM osthole or vehicle for 20 min. (**B**) A concentration-response curve for osthole-induced relaxation of 0.3 μM ACh–preconstricted airways. (**C**) Time course of relaxation of ACh-preconstricted airways in response to 10 μM osthole, nifedipine, or SB-366791. (**D**) Mouse PCLSs pretreated with 10 μM nifedipine, SB-366791, or vehicle for 30 min were constricted with 0.3 μM ACh (left) before exposure to 10 μM osthole to induce airway relaxation (right). (**E**) Concentration-response curves for albuterol (Alb)–induced relaxation of ACh-preconstricted airways in the presence of 0.3 μM osthole or vehicle. (**F**) Concentration-response curves for Alb- or osthole-induced relaxation of ACh-preconstricted airways in mouse PCLSs that were pretreated with vehicle or 100 μM Alb overnight (O/N) to induce β2-adrenoceptor desensitization. All data (means ± SEM) were generated from at least seven lung slices from four mice for each group (*$P < 0.05$, using ANOVA with the Bonferroni correction for multiple comparisons test).

Fig. 2. Osthole ameliorates AHR in mice. (**A** and **B**) Effect of the oral administration of osthole on AHR as assessed by lung resistance (R_L) induced by different doses of aerosolized MCh in HDM-sensitized mice (A) and naïve RGS2 KO mice (B). Top: Experimental scheme. Mice were treated by gavage vehicle or osthole (2.5 mg/10 g of body weight) 1 hour before MCh challenge. Data are means ± SEM ($n = 4$ for HDM-treated mice and $n = 6$ for RGS2 KO mice) and were analyzed using ANOVA with the Bonferroni correction for multiple comparisons test. *$P < 0.05$ and **$P < 0.01$ as compared with vehicle group.

it was similar to that in control mice (Fig. 2A). We and others reported that deletion of the *RGS2* gene leads to spontaneous AHR in mice (*22*, *23*). A single dose of osthole also significantly reduced lung resistance to MCh challenge in RGS2 KO (knockout) mice (Fig. 2B).

Osthole stimulates cAMP accumulation to activate PKA in human ASM cells

ASM contraction is directly responsible for airway constriction and AHR (*24*). Phosphorylation of myosin regulatory light chain 2 (MLC2) at Thr[18] and Ser[19] by myosin light chain kinase contributes to ASM contraction (*25*). Pretreatment with osthole (3 μM) prevented ACh-induced MLC2 phosphorylation in human ASM cells (Fig. 3A). Using a cAMP-dependent luciferase reporter assay, we found that treatment of human ASM cells with 0.1 μM osthole or 3 μM adenylyl cyclase activator forskolin for 48 hours increased cAMP levels by 3.2- or 4.5-fold, respectively (Fig. 3B). Increased cAMP activates PKA to induce ASM relaxation, and vasodilator-stimulated phosphoprotein (VASP) is a major substrate of PKA (*26*). Treatment of human ASM cells with osthole increased VASP phosphorylation at Ser[157] in a concentration-dependent manner (Fig. 3C), plateauing at 3 μM, which was blocked by the cell-permeable PKA inhibitor PKI or H89 (Fig. 3D).

Osthole potentiates albuterol-induced VASP phosphorylation and maintains its stimulatory effect on VASP phosphorylation in β2-adrenoceptor desensitized human ASM cells

Treatment with albuterol also induced VASP phosphorylation in human ASM cells, which was further enhanced when combined with 0.1 μM osthole (Fig. 3E). Pre-exposure to albuterol overnight caused β2-adrenoceptor desensitization in human ASM cells because reexposure of these cells to albuterol failed to increase VASP phos-

phorylation (Fig. 3F). However, osthole could still stimulate VASP phosphorylation despite β2-adrenoceptor desensitization in human ASM cells (Fig. 3F).

## Osthole augments EP2- and EP4-mediated autocrine PGE2 signaling in human ASM cells

Major determinants of cAMP levels in ASM include autocrine or paracrine stimulation by PGE2 through the receptors EP2 and EP4, β2-adrenoceptor stimulation by the sympathetic nervous system, and PDE activity (*9*). The β-adrenoceptor blocker propranolol attenuated albuterol-induced but not osthole-induced VASP phosphorylation (Fig. 4A). In contrast, the EP2 antagonist PF-04418948 and EP4 antagonist ONO-AE3-208 each partially inhibited osthole-induced VASP phosphorylation, and their combination completely abolished this phosphorylation in human ASM cells (Fig. 4B). Human ASM cells constitutively produce and secrete PGE2. We found that PGE2 secretion from human ASM cells in serum-free medium was not affected by treatment with osthole (3 μM). As expected, pretreatment with indomethacin or diclofenac, general inhibitors of COX enzymes, decreased PGE2 secretion by 95% (Fig. 4C). Pretreatment with indomethacin or diclofenac also abolished osthole-induced VASP phosphorylation in human ASM cells (Fig. 4D), suggesting that the effects of osthole may depend on PGE2 synthesis and secretion from human ASM cells. Thus, we further examined the ability of osthole to induce VASP phosphorylation in human embryonic kidney (HEK)–293 cells that do not produce endogenous PGE2 (*27*). Treatment with osthole alone did not induce VASP phosphorylation but enhanced exogenous PGE2–induced VASP phosphorylation in HEK-293 cells in a statistically significant manner, which was abolished by combined blockade of EP2 and EP4 (Fig. 4E). Osthole also augmented forskolin-induced VASP phosphorylation, which was insensitive to EP2 and EP4 inhibition (Fig. 4E). Furthermore, combined blockade of EP2 and EP4 attenuated the ability of osthole to stimulate the exogenous PGE2 but not the forskolin response in HEK-293 cells (Fig. 4F). These data suggest that osthole augments autocrine PGE2-stimulated, EP2- and EP4-dependent cAMP signaling in human ASM cells.

Osthole-induced relaxation of mouse small airways depends on endogenous PGE2 release

The β-adrenoceptor antagonist propranolol did not affect osthole-induced airway relaxation in mouse PCLS (Fig. 5A), but a combination of EP2 and EP4 antagonists caused a 12.7-fold rightward shift of the EC_{50} value for osthole-induced airway relaxation (Fig. 5B). Indomethacin or diclofenac also shifted the osthole relaxation curve rightward (Fig. 5C). Mouse PCLSs constitutively release PGE2, which is blocked by pretreatment with indomethacin or diclofenac. Treatment with osthole for 30 min did not affect the release of PGE2 from mouse PCLS (Fig. 5D). Thus, osthole-induced relaxation of mouse small airways depends on autocrine and/or paracrine stimulation by endogenous PGE2, similar to that observed in human ASM cells.

PDE4 controls autocrine PGE2 signaling in ASM cells

Several PDE isoforms including PDE3, PDE4, and PDE8 have been found in human ASM cells and control G_s-coupled receptor–stimulated intracellular cAMP signaling (*9*, *28*). Thus, we compared the abilities of osthole and the PDE4 inhibitor rolipram [median inhibitory concentration (IC_{50}) ~0.24 μM], the PDE3 inhibitor
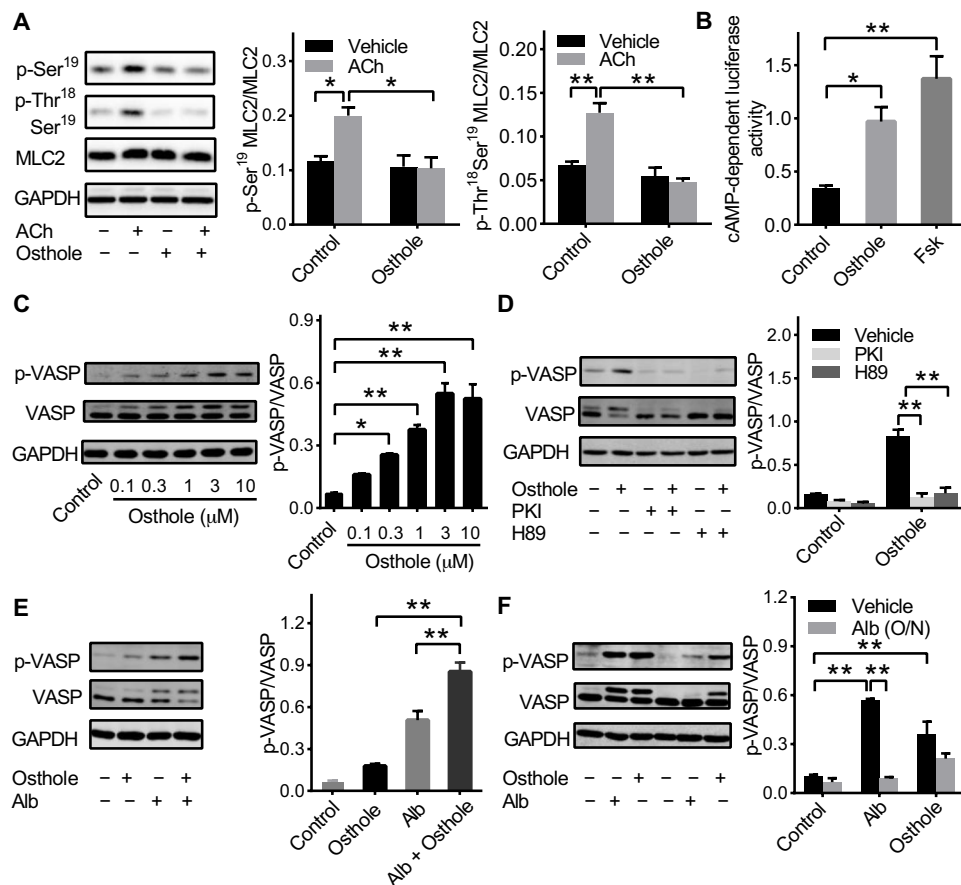
Fig. 3. Osthole stimulates cAMP accumulation to activate PKA in human ASM cells. (**A**) MLC2 phosphorylation in human ASM cells pretreated without (control) or with 3 μM osthole for 20 min and stimulated with 1 μM ACh or vehicle for 2 min. (**B**) cAMP-dependent luciferase activities in human ASM cells stimulated without (control) or with 0.1 μM osthole or 3 μM forskolin (Fsk). (**C**) VASP phosphorylation in human ASM cells stimulated with osthole for 15 min. (**D**) Osthole (3 μM)–stimulated VASP phosphorylation in human ASM cells pretreated with myristoylated PKI (10 μM), H89 (10 μM), or vehicle. (**E**) VASP phosphorylation in human ASM cells stimulated without (control) or with 0.3 μM osthole and/or 0.1 μM Alb. (**F**) Osthole (3 μM)–stimulated or Alb (1 μM)–stimulated VASP phosphorylation in human ASM cells pretreated with vehicle or 100 μM Alb overnight (O/N) to induce β2-adrenoceptor desensitization. Left: Representative Western blot; right: quantification of MLC2 or VASP phosphorylation by densitometry analysis, normalized to the signal for total MLC2 or VASP protein, respectively. All data are means ± SEM [(A), (B), (E), and (F), $n = 3$ separate experiments in one human ASM cell line; (C) and (D), $n = 3$ different human ASM cell lines, each experiment was repeated multiple times; *$P < 0.05$ and **$P < 0.01$, using ANOVA with the Bonferroni correction for multiple comparisons test]. GAPDH, glyceraldehyde-3-phosphate dehydrogenase.

pimobendane (IC_{50} of 0.32 μM), and the PDE8 inhibitor PF-04957325 ($IC_{50} < 10$ nM) (*29*) to stimulate VASP phosphorylation. Treatment with either osthole (3 μM) or rolipram (3 μM) alone statistically significantly increased VASP phosphorylation in human ASM cells, and the combination of osthole and rolipram did not have an additive effect. In contrast, neither pimobendane (3 μM) nor PF-04957325 (0.1 μM) was able to increase VASP phosphorylation in human ASM cells in a statistically significant manner (Fig. 6A). Treatment with rolipram increased cAMP-dependent luciferase activity in human ASM cells by 4.1-fold, whereas pimobendane or PF-04957325 had no significant effect (Fig. 6B). Rolipram also induced a rapid and prolonged relaxation of ACh-preconstricted airways (Fig. 6C) and potentiated albuterol-induced airway relaxation in mouse PCLS (Fig. 6D), similar to the effects of osthole (Fig. 1, C and E).

These data suggest that PDE4 is the predominant isoform controlling autocrine PGE2 signaling in ASM cells and that osthole may directly inhibit PDE4 to increase cAMP levels to trigger airway relaxation.

PDE4D mediates bronchodilation effects of osthole in vitro and in vivo

Among PDE4 isoforms, the physiological control of cAMP breakdown appears to be predominantly through the PDE4D splice variant in human ASM cells (*10, 11*). Thus, we investigated the effects of PDE4D knockdown on osthole-stimulated VASP phosphorylation in human ASM cells. PDE4D-specific small interfering RNA (siRNA), but not scrambled siRNA, reduced PDE4D mRNA expression by more than 70% (Fig. 7A) and abolished osthole-stimulated but not the non-selective PDE inhibitor 3-isobutyl-1-methylxanthine (IBMX)–stimulated VASP phosphorylation in human ASM cells (Fig. 7B). We also used the PDE4D-specific inhibitor GEBR-7b (*30*) to block endogenous PDE4D activity, which increased VASP phosphorylation in human ASM cells (Fig. 7C) and induced relaxation of ACh-preconstricted airways in mouse PCLS (Fig. 7D), similar to the effects of osthole. The combination of GEBR-7b and osthole did not have additive effects on VASP phosphorylation in human ASM cells (Fig. 7C) and airway relaxation (Fig. 7D). Bronchodilation rescue assays in mice showed that after preconstriction of airways with a maximal dose of MCh (150 mg/ml), aerosolization of either osthole and GEBR-7b (10 μg/10 g of body weight) alone into mouse lungs decreased lung resistance by a similar extent, and there was no additive effect (Fig. 7, E and F). In contrast, adding albuterol after osthole or GEBR-7b resulted in a further decrease in lung resistance (Fig. 7G). Together, these data suggest that PDE4D in ASM is the major target of osthole in vivo.

Osthole inhibits PDE4D5 activity in vitro
Of the PDE4D splice variants, PDE4D5 appears to be of particular functional importance in regulating cAMP levels in human ASM cells (*11*). Therefore, we examined the effects of osthole on the activity of PDE4D5 in vitro. Consistent with previous reports (*31*), the S126D mutant form of PDE4D5 displayed constitutive enzymatic activity, whereas the S126D-D556A double mutant had no enzymatic activity (Fig. 8A). Osthole inhibited the enzymatic activity of the PDE4D5 S126D mutant in a concentration-dependent manner
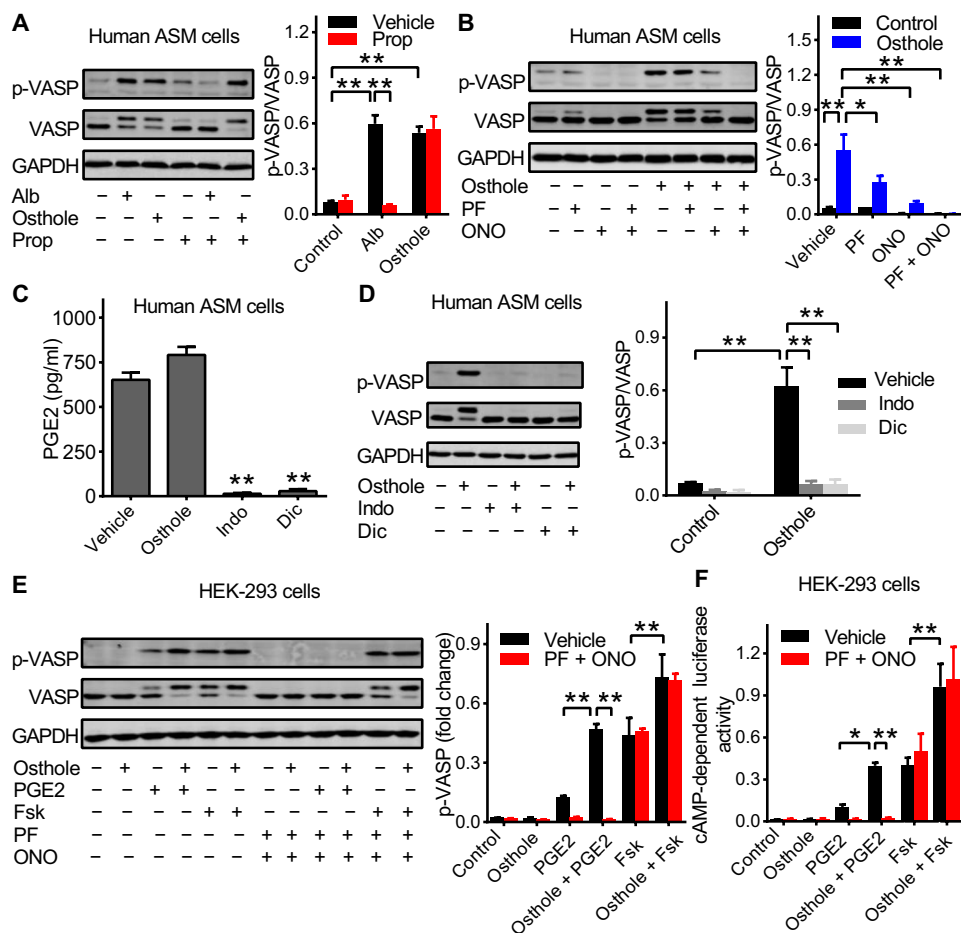
Fig. 4. Osthole augments EP2- and EP4-mediated autocrine PGE2 signaling in human ASM cells. (**A** and **B**) VASP phosphorylation in human ASM cells stimulated without (control) or with Alb (1 μM) or osthole (3 μM) for 15 min in the absence (vehicle) or presence of propranolol (Prop; 1 μM) (A) or PF-04418948 (PF; 0.3 μM) and/or ONO-AE3-208 (ONO; 0.3 μM) (B). (**C**) PGE2 secretion from human ASM cells in 30 min in the absence (vehicle) or presence of osthole (10 μM), indomethacin (Indo; 15 μM), or diclofenac (Dic; 10 μM). (**D**) Osthole (3 μM)–stimulated VASP phosphorylation in human ASM cells pretreated without (vehicle) or with Indo (15 μM) or Dic (10 μM). (**E** and **F**) HEK-293 cells were stimulated without (control) or with osthole (3 μM), PGE2 (0.1 μM), Fsk (3 μM), osthole + PGE2, or osthole + Fsk in the absence (vehicle) or presence of PF + ONO. Representative blot (left) and quantification (right) of VASP phosphorylation (E) and cAMP-dependent luciferase activity assays (F). All data are means ± SEM [(A), (B), and (D), $n = 3$ different human ASM cell lines; (C), (E), and (F), $n = 3$ separate experiments with one human ASM or HEK-293 cell line; $*P < 0.05$ and $**P < 0.01$ using ANOVA with the Bonferroni correction for multiple comparisons test].

with ~70% inhibition at 10 μM, similar to the inhibitory effect of 10 μM rolipram (Fig. 8B).

The crystal structure reveals that osthole binds to the PDE4D5 catalytic domain

We solved the crystal structure of the PDE4D5 catalytic domain complexed with osthole at 2.3 Å resolution. There are four molecules of the PDE4D5 catalytic domain in the crystallographic asymmetric unit in the space group of $P2_12_12_1$, and osthole is located at the active pocket of each molecule (Fig. 8C). Osthole is a natural coumarin (Fig. 8D) and fits well into the 2Fo − Fc electron density maps calculated from the structures omitting osthole and contoured at 1.5σ (Fig. 8D). The O-1 of osthole forms a hydrogen bond of 3.3 Å with the amide nitrogen of the Gln[607] side chain, the O-2 of osthole forms a hydrogen bond of 2.9 Å with the hydroxy of the Thr[571] side

chain, and the coumarin ring is sandwiched between the hydrophobic residues of Phe[610] and Phe[578]/Ile[574] (Fig. 8E). In addition, osthole interacts with Tyr[397], Asn[559], Met[595], and Ser[606] of PDE4D5 through hydrophobic interactions.

### The upstream conserved region 2 of PDE4D5 increases the binding affinity of osthole

A high-affinity rolipram binding site (HARBS) in the upstream conserved region 2 (UCR2) of PDE4 is also involved in binding of rolipram-type PDE4 inhibitors (32). Osthole was docked into the UCR2 capped PDE4D catalytic pocket by superposition of our structure and a reported structure of the PDE4D catalytic domain and UCR2 regulatory helix (6BOJ) (33) with the root mean square deviation of 0.4 Å. Phe[268] of HARBS interacts with Phe[578] and Met[595] in the catalytic pocket through hydrophobic bonds. However, there is no direct interaction between the UCR2 and osthole (Fig. 8F). When comparing the inhibitory effects of osthole on the full-length PDE4D5/S126D and its catalytic domain, there was a 43.8-fold leftward shift of IC50 (Fig. 8G). Mutation of Phe[268] to Ala in PDE4D5/S126D (termed as S126D-F268A) also significantly reduced the osthole inhibitory effect with an IC50 of 16.8 ± 0.41 μM, close to the IC50 value of the catalytic domain. Thus, HARBS does not interact with osthole directly but increases the binding affinity of osthole to the PDE4D5 catalytic domain.

DISCUSSION

Using an integrated multimodal approach, we demonstrated that osthole functioned as a PDE4D inhibitor to amplify autocrine PGE2 signaling in ASM cells to induce cAMP/PKA-dependent relaxation of small airways. Moreover, our modeling studies identified osthole binding sites on PDE4D5, which provides a new molecular target to guide the development of novel therapeutics for asthma.
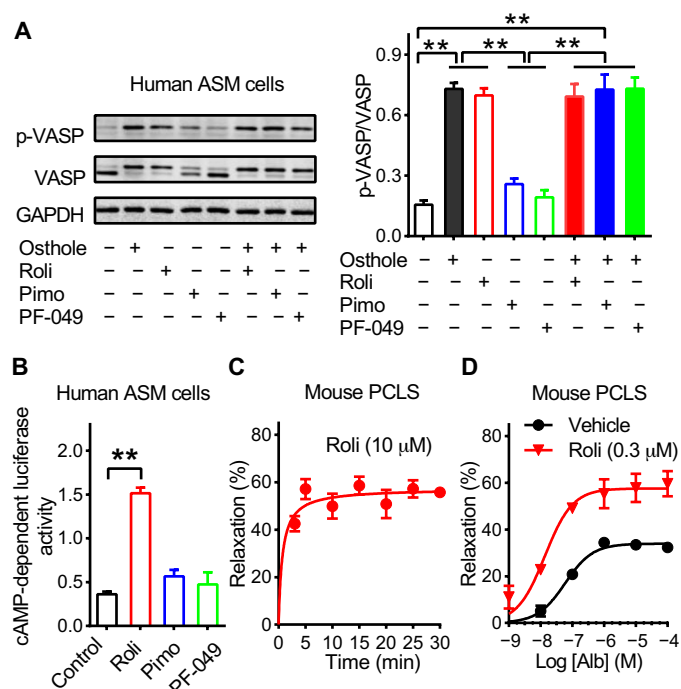
Osthole antagonized ACh-mediated airway constriction in mouse PCLS in a concentration-dependent manner. Acute treatment with osthole also induced a rapid relaxation of preconstricted airways of mouse PCLS ex vivo. AHR is exaggerated constriction of the airways in response to various bronchoconstrictors. It is a key diagnostic criterion of asthma, and improvement in AHR is associated with better asthma control (34). A single dose of osthole administrated by gavage attenuated both HDM-induced and RGS2 deficiency–induced AHR in mice, suggesting a potential application of osthole as a bronchoprotective and bronchodilator agent to treat asthma. The
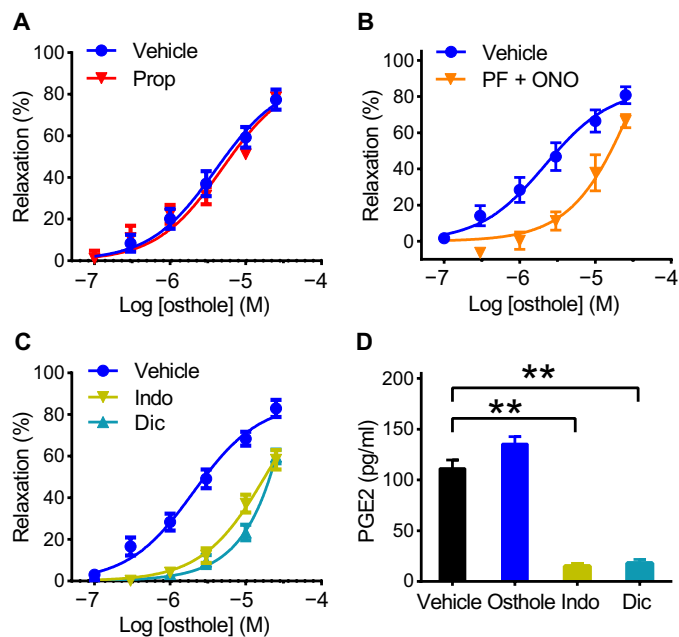
Fig. 5. Osthole relaxation of small airways in mouse PCLS depends on endogenous PGE2. (**A** to **C**) Concentration-response curves for osthole-induced relaxation of ACh-preconstricted airways in mouse PCLS preincubated without (vehicle) or with 1 µM Prop for 30 min (A), 0.3 µM PF plus 0.3 µM ONO for 30 min (B), 15 µM Indo, or 10 µM Dic for 1 hour (C). Relaxation was calculated as percent relaxation after submaximal airway constriction in 0.3 µM ACh-treated PCLS. (**D**) PGE2 release from mouse PCLS in 30 min in the absence (vehicle) or presence of osthole (10 µM), Indo (15 µM), or Dic (10 µM). Relaxation data (means ± SEM) were generated in at least six lung slices from four mice for each group. PGE2 release data (means ± SE) were generated from three mice for each group (four pieces of PCLS per mouse). **P < 0.01 using ANOVA with the Bonferroni correction for multiple comparisons test.

Fig. 6. PDE4 controls autocrine PGE2 signaling in ASM cells and regulates airway relaxation in mouse PCLS. (**A**) VASP phosphorylation in human ASM cells stimulated without (control) or with osthole (3 µM), rolipram (Roli; 3 µM), pimobendane (Pimo; 3 µM), PF-04957325 (PF-049; 0.1 µM), and combinations of two drugs as indicated for 15 min. (**B**) cAMP-dependent luciferase activities in human ASM cells treated without (control) or with Roli, Pimo, or PF-049. (**C**) Relaxation of 0.3 µM ACh–preconstricted airways in mouse PCLS in response to 10 µM Roli. (**D**) Concentration-response curves for Alb-induced relaxation of ACh-preconstricted airways in the presence of 0.3 µM Roli or vehicle. Data shown are means ± SEM [(A), n = 3 different ASM cell lines; (B), n = 3 separate experiments in one human ASM cell line; **P < 0.01 using ANOVA with the Bonferroni correction for multiple comparisons test]. Data shown in (C) and (D) were generated in at least six lung slices from three mice for each group.

β2-adrenoceptor agonist albuterol is widely used as an acute bronchodilator in the clinic, but its overuse can lead to desensitization of β2-adrenoceptors leading to suboptimal bronchodilation (*3*). Osthole not only markedly potentiated albuterol-induced bronchodilation effects but also could cause airway relaxation even after desensitization of β2-adrenoceptors. Thus, our results are especially interesting because of their clinical relevance to patients presenting with excessive bronchoconstriction whom are poorly responding to albuterol rescue therapy.

Osthole has been reported to block L-type $Ca_v1.2$ and TRPV1 calcium channel activity. Although ACh-induced bronchoconstriction can be antagonized by nifedipine or SB-366791, relaxation due to osthole was distinguished by its greater magnitude and achievement of its maximum response within seconds rather than tens of minutes. Moreover, osthole caused similar relaxation in airways pretreated or not with either nifedipine or SB-366791. These results indicate that osthole-induced airway relaxation was independent of direct inhibition of these two calcium channels. Phosphorylation of MLC2 in response to bronchoconstrictors such as ACh is an index for the activation of ASM contraction that is directly responsible for airway constriction and AHR. We found that ACh-induced phosphorylation of MLC2 in human ASM cells was blocked by osthole, suggesting that osthole directly targets ASM cells. Current clinical treatment for asthma uses β2-adrenoceptor agonists to activate adenylyl cyclase to increase cAMP levels, which can activate PKA to

phosphorylate various target proteins to induce ASM relaxation (*6*). Osthole increased cAMP levels in human ASM cells and augmented PKA-dependent responses, which can happen either by receptor-dependent adenylyl cyclase activation or by blocking the breakdown of cAMP through inhibition of PDEs.

Similar to β2-adrenoceptor agonists, prostaglandins also play an important role in airway relaxation. PGE2, the major prostaglandin product in the lower respiratory microenvironment, is synthesized and secreted by multiple cells in the lungs (*35*). Inhibition of prostaglandin synthesis by aspirin was one of the first endotypes of asthma to be identified (*36*). Thus, it was plausible that osthole stimulated G_s-coupled prostaglandin receptors EP2 or EP4 to increase intracellular cAMP. We found that osthole-induced VASP phosphorylation in ASM cells was insensitive to β-blockade. Although either the EP2 or EP4 antagonist partially attenuated osthole-induced VASP phosphorylation in human ASM cells, the EP4 antagonist was more effective, and a combination of EP2 and EP4 antagonists abolished the effect of osthole. There is ongoing debate over the role of EP2 and EP4 in mediating the effects of PGE2 in ASM from different species. Buckley *et al.* (*37*) demonstrated that EP2 mediates the bronchodilator activity of PGE2 in guinea pig, murine, and monkey
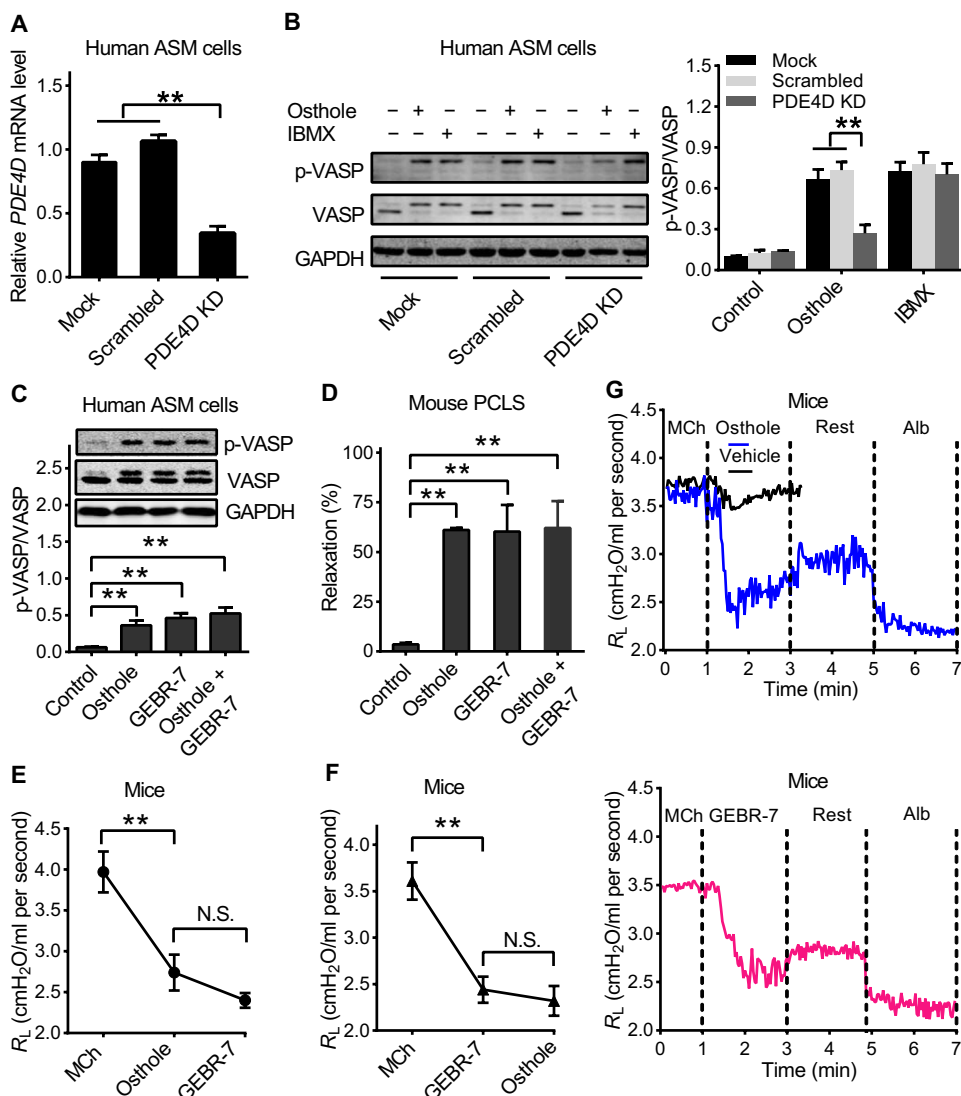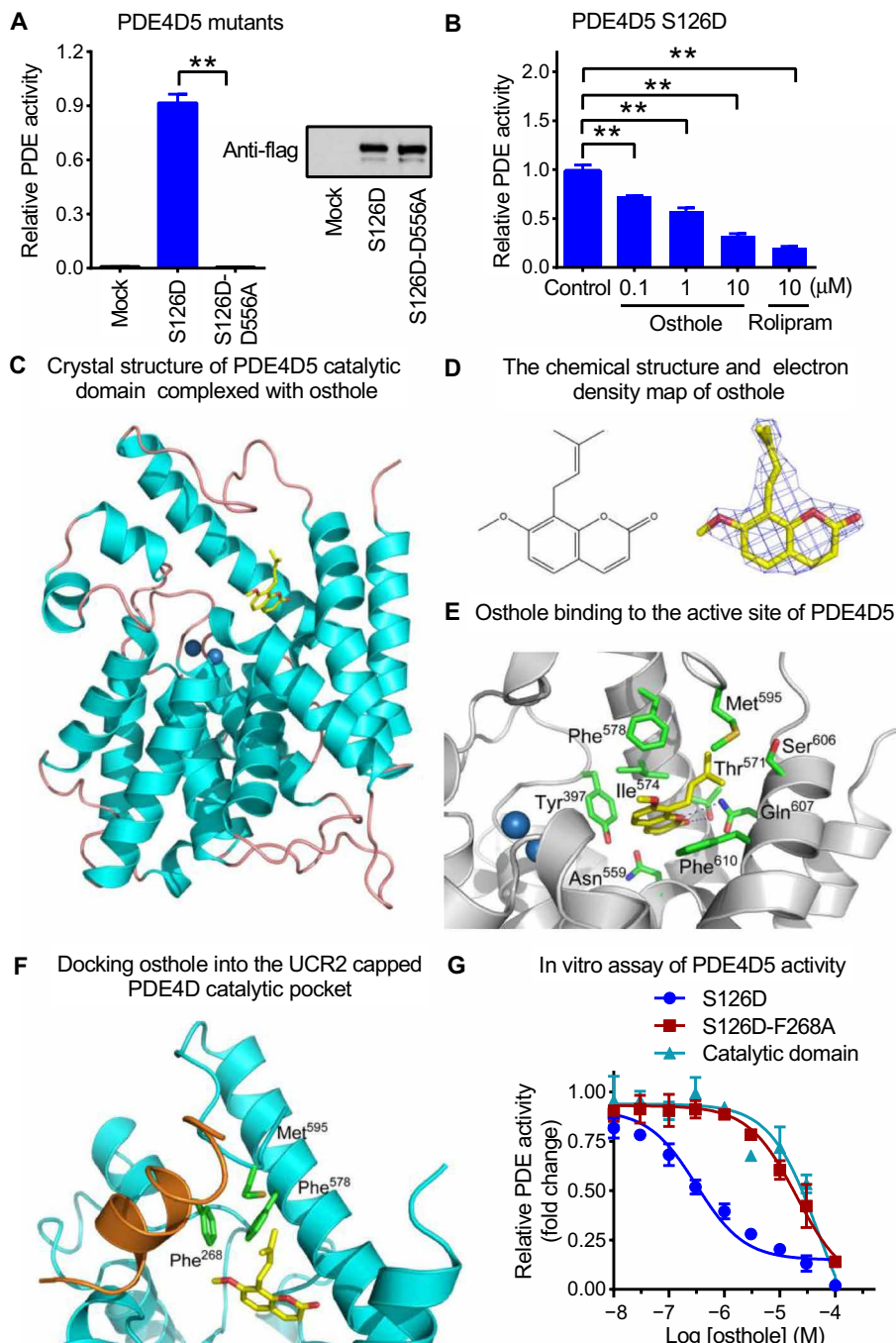
Fig. 7. Osthole exerts its bronchodilation effects through PDE4D in vitro and ex vivo. (A and **B)** Human ASM cells were transfected without (mock) or with scrambled or PDE4D siRNA. Cells were subjected to quantitative RT-PCR analysis of relative *PDE4D* mRNA expression (A) and Western blot analysis of VASP phosphorylation stimulated without (control) or with osthole (3 μM) or IBMX (500 μM) for 15 min (B). **(C)** VASP phosphorylation in human ASM cells stimulated without (control) or with 3 μM osthole, 10 μM GEBR-7, or the combination of drugs. The data are means ± SEM (*n* = 3 different ASM cell lines). **(D)** Relaxation of 0.3 μM ACh–preconstricted airways induced by vehicle (control), 10 μM osthole, 25 μM GEBR-7, or the combination of drugs in mouse PCLS. The data (means ± SEM) were generated in at least five PCLS from three mice for each group. **(E** to **G)** Mouse airways were preconstricted with MCh (150 mg/ml). Ten microliters of osthole (2.5 mg/ml) before (E) or after GEBR-7b (2.5 mg/ml) (F) was sequentially aerosolized over 30 s to assess bronchodilator rescue as indicated by the average decrease in lung resistance (*R*$_L$) 2 min after aerosol administration. (G) Representative time course of bronchodilator rescue of Alb (10 μl, 2.5 mg/ml) aerosolized into mouse lungs after osthole or GEBR-7b. *N* = 4 mice for each group in each experiment. **P < 0.01 using the Kruskal-Wallis test (A); **P < 0.01 using ANOVA with the Bonferroni correction for multiple comparisons test (B to F) and N.S. for nonsignificance (E and F). KD, knockdown.

trachea, whereas EP4 mediates bronchodilator activity of PGE2 in human airways. In contrast, Michael *et al.* (*38*) showed that both EP2 and EP4 are functionally important in inhibiting human ASM cell proliferation. Our data are consistent with the notion that osthole exerts its bronchodilation effects through both EP2 and EP4. However, our data did not discern between a direct agonist effect or an indirect effect of osthole. ASM is thought to be an important

source of PGE2 in airway tissue (*39*). We found that both human ASM cells and mouse PCLS constitutively produce and secrete PGE2, which is largely blocked by treatment with general COX inhibitors, consistent with the notion that COX enzymes are required for PGE2 synthesis (*40*). Because osthole can induce a rapid and prolonged airway relaxation, it is possible that osthole is activating COX-dependent PGE2 release that helps drive these kinetics and efficacy. However, we found that the amount of PGE2 released from human ASM cells and mouse PCLS is enough to activate EP2 and EP4, and treatment with osthole did not affect PGE2 release. In HEK-293 cells, which express EP2 and EP4 but do not synthesize prostaglandins, osthole treatment potentiated VASP phosphorylation to exogenous PGE2 without affecting VASP phosphorylation, and both the basal and osthole-potentiated responses were abolished by the combination of EP2 and EP4 antagonists. These data indicated that prostaglandin synthesis was required for the osthole response, which was confirmed in human ASM cells when the osthole response was abolished with general COX inhibitors. Similarly, large rightward shifts of the osthole relaxation concentration-response curve in mouse PCLS were caused by EP2/EP4 receptor blockade or prostaglandin synthesis inhibition, whereas the β-blocker propranolol had no effect.

Osthole did not affect basal VASP phosphorylation in HEK-293 cells, but it did potentiate VASP phosphorylation by forskolin. This result suggests PDE inhibition as a mechanism mediating the effect of osthole. We found that treatment with either osthole or the PDE4 inhibitor rolipram, but not inhibitors of PDE3 or PDE8, significantly increased VASP phosphorylation in human ASM cells, and a combination of osthole and rolipram did not have additive effects. Our results are consistent with previous reports that inhibitors of PDE4, but not of PDE3, increase β2-agonist effects

(*41*) and that PDE8 does not inhibit EP2/EP4 signaling in human ASM cells (*28*). Rolipram also induced rapid and prolonged airway relaxation and potentiated albuterol-induced airway relaxation in mouse PCLS, similar to the effects of osthole. These data suggest that PDE4 is the predominant isoform controlling autocrine PGE2 signaling in ASM cells and that osthole may directly inhibit PDE4 to increase cAMP levels to trigger airway relaxation. Our results are

A — PDE4D5 mutants

B — PDE4D5 S126D

C — Crystal structure of PDE4D5 catalytic domain complexed with osthole

D — The chemical structure and electron density map of osthole

E — Osthole binding to the active site of PDE4D5

F — Docking osthole into the UCR2 capped PDE4D catalytic pocket

G — In vitro assay of PDE4D5 activity

Fig. 8. Osthole inhibits PDE4D5 activity, and the crystal structure of the PDE4D5 catalytic domain complexed with osthole. (**A**) PDE activities (left) and representative Western blot (right) of c-Flag–tagged recombinant PDE4D5-S126D (active) and PDE4D5-S126D-D556A (enzymatically dead) mutants. (**B**) Inhibition of the enzymatic activity of PDE4D5-S126D by osthole or 10 μM rolipram. Data in (A) and (B) are means ± SEM ($n = 3$ separate experiments in technical duplicate, **$P < 0.01$, using ANOVA with the Bonferroni correction for multiple comparisons test). (**C**) Ribbon diagram of the monomeric PDE4D5 catalytic domain complexed with osthole (oxygen, red; carbon, yellow) and with divalent metals (blue balls) for reference. (**D**) The chemical structure of osthole and electron density map of osthole. The omitted (2Fo – Fc) map was contoured at 1.5σ. (**E**) Osthole binding to the active site of PDE4D5. The coumarin group forms two hydrogen bonds with Gln[607] and Thr[571] (dotted lines). The protein side-chain atoms are colored as follows: oxygen, red; nitrogen, blue; sulfur, yellow; and carbon, green. (**F**) Docking osthole into the UCR2 capped PDE4D catalytic pocket. UCR2 is colored orange, and catalytic domain residues are colored cyan. (**G**) Concentration-response curves of osthole inhibition of PDE activities of PDE4D5-S126D, HARBS mutant (S126D-F268A), and the catalytic domain of PDE4D5 (317-676). Data shown are means ± SE ($n = 3$ separate experiments in technical duplicate).

consistent with a previous report that osthole attenuates neutrophilic oxidative stress and hemorrhagic shock–induced lung injury by inhibiting PDE4 (*42*). Specifically, knockdown of endogenous PDE4D abolished osthole-stimulated VASP phosphorylation in human ASM cells, although it did not increase basal VASP phosphorylation. This effect was presumably due to compensation of other osthole-insensitive PDE isoforms because the nonselective PDE inhibitor IBMX increased VASP phosphorylation in human ASM cells with PDE4D knockdown. Furthermore, we found that nebulization of either osthole or the PDE4D-specific inhibitor GEBR-7b into mouse lungs induced bronchodilation rescue by a similar extent, and there was no additive effect. Together, these data suggest that PDE4D in ASM is the major target of osthole in vivo.

At least 11 different splice variants or isoforms of PDE4D that share the same catalytic domain have been identified (*43*). We used PDE4D5 as a model to investigate whether osthole directly inhibits PDE4D activity because it regulates cAMP levels in human ASM cells (*11*). Osthole concentration dependently inhibited the activity of the constitutively active PDE4D5 S126D mutant. X-ray crystallography analysis showed that osthole directly bound to the active site of PDE4D5. Previous crystallographic data indicate that this active site includes a compact α-helical structure that contains a metal binding pocket (M pocket), a solvent-filled side pocket (S pocket), and a pocket referred to as the Q pocket (*44*). The Q pocket consists mainly of hydrophobic residues for tight stacking of the planar ring structure of nucleotides by hydrophobic interaction and contains an important conserved Gln residue for nucleotide recognition through hydrogen bonds (*45*). In our study, we observed that osthole bound to the Q pocket and formed a hydrogen bond with the conserved Gln[607]. Osthole also formed a hydrogen bond with Thr[571], which may confer an additional inhibitory effect and/or recognition ability. The Q pocket is the binding site for the adenine group of cAMP in PDE4D where the N-1 of adenine forms a hydrogen bond with Gln[607] for recognition, and like osthole, cAMP also binds to residues Met[595], Ile[574], Phe[610],
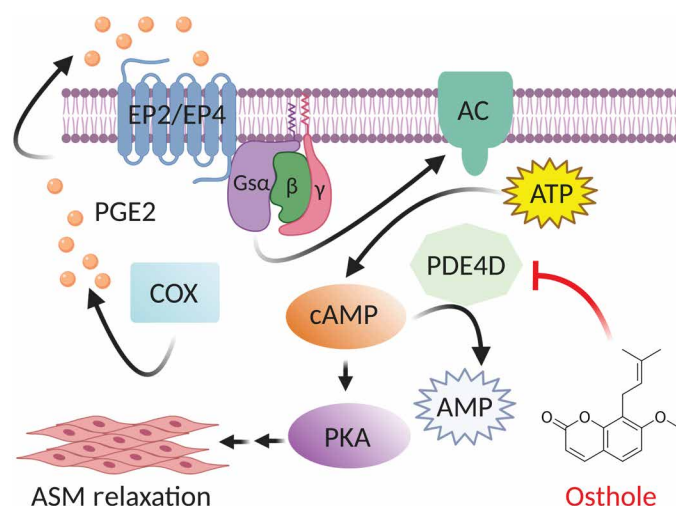
and Asn[559] through hydrophobic interactions. Because the Q pocket is a narrow region, its occupancy by osthole should competitively prevent cAMP binding and hydrolysis. Phe[268], which extends from the UCR2, can form a network of interactions with the allosteric modulator type inhibitors or hydrophobic residues to modulate PDE4 activity (46). Molecular docking results suggest that osthole did not interact directly with the high-affinity binding site of the prototypical PDE4 inhibitor rolipram on PDE4D. However, deletion of the UCR2 domain or mutation of Phe[268] significantly reduced the osthole inhibitory effect. Thus, the UCR2 nevertheless acted to increase the binding affinity of osthole to PDE4D5, which may be due to a weak interaction between osthole and the catalytic pocket until the UCR2 closes and enhances the hydrophobic interaction in the catalytic domain to lock osthole firmly in place.

Together, these data demonstrate that osthole augments autocrine PGE2–mediated relaxation of airways by blocking PDE4D activity in ASM. Blockade of PDE4D activity increases intracellular cAMP levels with subsequent stimulation of PKA that leads to ASM relaxation and bronchodilation (Fig. 9). The speed and efficacy of the reversal of airway constriction by osthole suggest that it or similar drugs could treat asthma, especially β2-adrenoceptor agonist–resistant asthma. In addition, osthole increases both the apparent potency and efficacy of albuterol. Thus, a combination of osthole and β2-adrenoceptor agonists could be a superior treatment strategy for asthma. This approach could limit adverse effects of β2-adrenoceptor agonists. Osthole has been used for medicinal purposes and is well tolerated at lower doses (47), in contrast to other currently available PDE4 inhibitors that have considerable adverse effects. Osthole is a pleiotropic agent, presumably because it also targets PDEs expressed in different tissues. This may limit its usefulness for chronic treatment of asthma unless delivered directly to the airways. The potential for administration by inhalation offers the possibility of diminishing adverse effects of osthole-like medications. In our studies, we found that aerosolized osthole at 10 μg/10 g of body weight, 250-fold lower than the typical oral dose, had a bronchodilator rescue effect in mice. By potentiating the effects of locally synthesized and released prostaglandins, the short half-life of prostaglandins themselves is less of a concern, and when osthole or its congeners are administered systemically, widespread adverse effects can also be avoided. This local low-dose drug application should minimize unwanted systemic side effects. Furthermore, the information about how osthole binds to the PDE4D5 catalytic domain as revealed by the crystal structure allows us to chemically modify osthole to increase its potency while reducing its side effects. Given that β2-agonist–resistant asthma contributes to a substantial number of asthma fatalities, osthole-like drugs that promote prostaglandin-mediated bronchodilation could play a major role in treating drug-resistant and poorly controlled asthma.

Fig. 9. A proposed molecular mechanism underlying osthole-induced airway relaxation. ASM cells secrete PGE2 that activates G_s-coupled EP2 and EP4 to stimulate adenylyl cyclase (AC) to produce cAMP that is rapidly degraded by PDE4D in ASM cells. Osthole inhibits PDE4D activity to amplify autocrine PGE2 signaling to increase cAMP levels in ASM cells, leading to cAMP/PKA-dependent, ASM-mediated airway relaxation.

MATERIALS AND METHODS
Reagents and cells
Hanks' balanced salt solution supplemented with 20 mM Hepes buffer, penicillin, and streptomycin was purchased from Invitrogen. VASP and MLC2 antibodies were purchased from Cell Signaling Technology Inc. Osthole with a purity greater than 98% was purchased from Ark Pharm. Albuterol was purchased from Selleck Chemicals. Forskolin was purchased from Absin Bioscience. PGE2 was purchased from TCI Development Co. Ltd. Nifedipine, SB-36679001, rolipram,

pimobendane, PF-04957325, H89, and propranolol were purchased from MedChem Express. Myristoylated PKI (14-22) was from Tocris Bioscience. PF-04418948, ONO-AE3-208, indomethacin, and diclofenac were purchased from Cayman Chemical. GEBR-7b was from Millipore Sigma. Unless indicated otherwise, other reagents were purchased from either Sigma-Aldrich or Thermo Fisher Scientific. Three human ASM cell lines were used. These cell lines were established by Panettieri's laboratory using human lung tissue samples obtained from nonasthmatic donors during open-lung resection at the time of death (48). Cells were cultured at 37°C with 5% CO_2 in smooth muscle cell growth medium from Genlantis containing antibiotics and antimycotic. Cells were seeded in Dulbecco's modified Eagle's medium (DMEM)/F-12 medium (Hyclone) supplemented with 10% fetal bovine serum for 24 hours. Serum was then removed before phosphorylation stimulation experiments. In all studies, cells were used at 60 to 80% confluence and passage numbers 3 to 8. African green monkey kidney COS7 [American Type Culture Collection (ATCC) CRL-1651] and HEK-293 (ATCC CRL-1573) cells were from the ATCC and cultured in DMEM medium with 10% fetal bovine serum. HEK-293 cells deficient in PGE2 synthesis (27) were used to analyze the effects of osthole on exogenous PGE2–induced cellular the prostaglandin E2 receptor (EP) signaling and cAMP production without any impact on secretion of endogenous PGE2 from cells.

Animal studies and drug administration
Mice used in our study were obtained by in-house breeding. D. Siderovski provided a RGS2 KO C57BL/6J mouse breeding colony. C57BL/6j female mice (10 to 12 weeks old) were exposed to 25 μg of purified HDM extract (Greer) in saline intranasally 4 days/week for 3 weeks. AHR of HDM-treated mice and naïve RGS2 KO mice was determined by direct measurement of lung resistance (R_L) in response to nebulized MCh in anesthetized, ventilated mice using a FinePointe apparatus (Buxco, Wilmington, NC, USA) as described

previously (*22*). A single dose of osthole (25 mg/ml, 0.1 ml/10 g of body weight) was administered by gavage 1 hour before MCh challenge. To assess bronchodilator rescue, C57BL/6j naïve mice were challenged with increasing doses of MCh (0 to 100 mg/ml). Maximum airway constriction, measured as R_L, was induced with a maximal concentration of MCh (150 mg/ml) to reach a stable lung resistance phase. A volume of 10 μl of osthole (2.5 mg/ml), GEBR-7b (2.5 mg/ml), albuterol (2.5 mg/ml), or vehicle was then aerosolized over 30 s sequentially to assess bronchodilator rescue as indicated by the average decrease in lung resistance 2 min after the aerosol was administered (*49*). All animal experiments were approved by the Creighton University Institutional Animal Care and Use Committee.

Airway constriction and relaxation of mouse PCLS
Mouse PCLSs were prepared as described previously (*22*). Lung slices with airways completely lined by epithelial cells with beating cilia were selected for study. Small airways of mouse PCLS with a diameter of 150 to 400 μm are typically used to evaluate the constriction-relaxation response ex vivo (*50*). In our study, mouse airways with averaged diameter of 280 ± 30 μm were used. The slices were placed on glass coverslips and airways visualized with an inverted microscope. Phase-contrast images were captured in time-lapse mode, and time-dependent changes in the cross-sectional areas of the airway lumen were measured by pixel summing using Image-Pro Plus software (Media Cybernetics Inc.). Constriction or relaxation was calculated on the basis of a decrease or increase in cross-sectional area of an airway (*22*). The experiments were performed at 37°C.

Desensitization of β2-adrenoceptors in human ASM cells and mouse PCLS
To desensitize β2-adrenoceptors, human ASM cells were seeded into 12-well plates at a density of 6×10^4 cells/ml in 10% fetal bovine serum–supplemented DMEM/F12 for 24 hours and then treated with 1 μM albuterol or vehicle control in DMEM/F12 overnight. To desensitize β2-adrenoceptors in airways, mouse PCLSs were incubated with 100 μM albuterol or vehicle control in DMEM overnight. Cells and PCLS were washed extensively to remove residual albuterol before exposure to albuterol or osthole.

Measurement of PGE2 secretion from human ASM cells and mouse PCLS by enzyme-linked immunosorbent assay
Human ASM cells were seeded into a 24-well plate at a density of 4×10^4 cells per well in DMEM/F-12 medium, whereas six pieces of mouse PCLS were cultured in 1 ml of DMEM medium. After overnight serum starvation, cells and PCLS were pretreated with indomethacin (15 μM), diclofenac (10 μM), or vehicle for 1 hour; changed to fresh medium; and treated with 10 μM osthole, 15 μM indomethacin, 10 μM diclofenac, or vehicle for 30 min. Conditioned media were collected and analyzed for PGE2 concentrations using a Prostaglandin E₂ Parameter Assay kit (KGE004B, R&D Systems Inc.). Conditioned medium from HEK-293 cells was used as the negative control.

cAMP-dependent luciferase reporter assays
HEK-293 cells or human ASM cells were cotransfected with the Renilla luciferase plasmid pRL-SV40P (Addgene) and firefly luciferase constructs under the transcriptional control of multiple units of the cAMP response element (pADneo2-C6-BGL) (*51*). Cells were treat-

ed without (control) or with reagents for 48 hours. Luciferase activities were measured using the dual-luciferase assay system (Promega). The results were presented as normalized firefly luciferase activity (firefly luciferase activity/Renilla luciferase activity).

Knockdown of PDE4D in human ASM cells by dual transfection of siRNA
Human ASM cells (1.2×10^5) were transfected without (mock) or with PDE4D siRNA (si-h-PDE4D_101) or scramble siRNA (siR NC #1) (RiboBio) using Lipofectamine RNAiMAX reagent (Invitrogen) according to the manufacturer's instructions. The final concentration of siRNA was 50 nM. After 24 hours, cells were re-transfected with the siRNAs as described above and cultured for additional 48 hours. Cells were subjected to quantitative reverse transcription polymerase chain reaction (RT-PCR) analysis of PDE4D mRNA expression as described (*11*).

Western blot
Protein was extracted from cells using 1× radioimmunoprecipitation assay lysis buffer with protease and phosphatase inhibitors. Protein samples were loaded on 10% SDS polyacrylamide gels, electrophoresed, and transferred onto polyvinylidene difluoride membranes. Protein bands recognized by primary antibodies were visualized by using secondary antibodies for the Odyssey IR imaging system (LI-COR Bioscience), and densitometry analysis was performed with Image Studio software as described (*48*). The signal for phosphorylated MLC2 or VASP was normalized to the signal for total MLC2 or VASP protein, respectively.

In vitro assay of PDE activity
PDE activity was determined with a PDELight HTS cAMP phosphodiesterase kit (Lonza) according to the manufacturer's instruction. One microliter of eukaryotically expressed PDE eluate or 10 ng of prokaryotically expressed PDE protein was incubated with osthole or rolipram for 20 min in PDE buffer (10 mM tris-HCl at pH 7.5). After the addition of 2 μM cAMP and an additional 1 hour of incubation, 10 μl of stop solution and 20 μl of AMP detection reagent were added. Ten minutes later, luminescence was measured with a Varioskan Flash (Thermo Fisher Scientific). All reactions were carried out at room temperature.

Expression of PDE4D5 protein in mammalian cells
COS7 cells were transfected with pcDNA3.1 encoding c-Flag–tagged PDE4D5-S126D (active) or PDE4D5-S126D-D556A (enzymatically dead) mutants and harvested 48 hours later in lysis buffer (50 mM tris-HCl at pH 7.4, 1% NP-40, 0.25% deoxycholate, 150 mM NaCl, and 1 mM EDTA, supplemented with protease inhibitor). Cell lysates were centrifuged at 12,000 rpm for 20 min to remove debris. Supernatants were immunoprecipitated with anti-FLAG M2 affinity beads (A2220; Sigma-Aldrich) and purified using desalting columns (Zeba Spin Desalting Columns; Thermo Fisher Scientific).

Expression and purification of PDE4D5 full length or its catalytic domain in *Escherichia coli*
Full-length human PDE4D5 active mutant S126D and mutant S126D-F268A were subcloned into expression vector pGEX-6P-1 and expressed in *E. coli* BL21(DE3) cells (Invitrogen). Cells were cultured at 37°C in LB medium until optical density at 600 nm (OD₆₀₀) reached 0.6. Then, 1 mM isopropyl β-D-thiogalactopyranoside (IPTG)

was added to induce protein expression at 30°C for 4 hours. The PDE4D5 mutant proteins were purified using glutathione *S*-transferase bind resin (Millipore Sigma), glutathione elution, precision protease cleavage, and Superdex 200 (Millipore Sigma) columns. The purified proteins were dissolved in 50 mM tris-HCl buffer (pH 8.0) with 100 mM NaCl and 1 mM β-mercaptoethanol and stored at −80°C. The catalytic domain of human PDE4D5 (317-676) was subcloned into the expression vector pET15b and expressed in *E. coli* BL21(DE3) cells. Cells were cultured at 37°C until OD_{600} reached 0.6, when 0.1 mM IPTG was added to induce protein expression at 15°C for 24 hours. The recombinant PDE4D5 catalytic domain was purified using Ni-NTA (nitrilotriacetic acid) affinity columns (Qiagen), thrombin cleavage, and Superdex 200 columns. PDE4D5 catalytic domain protein purity was greater than 95% as shown by SDS–polyacrylamide gel electrophoresis.

Crystallization and structure determination

Apo crystals of the PDE4D5 catalytic domain were grown by vapor diffusion with PDE4D5 catalytic domain (20 mg/ml) in buffer of 50 mM NaCl, 20 mM tris-HCl (pH 7.5), 1 mM β-mercaptoethanol, and 1 mM EDTA against a well solution of 0.1 M Hepes (pH 7.5), 18% polyethylene glycol 3350, 25% ethylene glycol, and 10% isopropanol at 4°C. To determine the location of the osthole-binding site, apo crystals were soaked with 10 mM osthole for 48 hours at 4°C with a final concentration of 2% dimethyl sulfoxide. Diffraction data were collected on the BL17U beamline of Shanghai Synchrotron Radiation Facility at a temperature of 100 K while using radiation of wavelength 0.9793 Å. The crystal-to-detector distance was set to 350 mm, and the oscillation angle was set to 0.5°. The exposure time was optimized to 0.2 s to balance the diffraction resolution and radiation damage. The diffraction datasets were indexed, merged, and scaled using the HKL2000 program suite (*52*). The structure was determined by the molecular replacement method with 1Q9M as the search model with program CCP4 and Phenix (*53*, *54*). The structure was refined by Phenix and Coot (*55*), and the PDE4D5 catalytic domain structure was lastly refined to 2.3 Å with an R_{work} of 18.7% and an R_{free} of 22.0%.

Data analysis

Data are expressed as means ± SEM. Groups were compared using a one-way or two-way analysis of variance (ANOVA) with the Bonferroni correction for multiple comparisons testing. The Kruskal-Wallis test was conducted for analysis of normalized data. A probability level (*P*) of 0.05 was used to determine statistical significance. GraphPad Prism software package was used for all statistical tests.

View/request a protocol for this paper from *Bio-protocol*.

REFERENCES AND NOTES

1. M. Johnson, The β-adrenoceptor. *Am. J. Respir. Crit. Care Med.* **158**, S146–S153 (1998).
2. S. C. Lazarus, H. A. Boushey, J. V. Fahy, V. M. Chinchilli, R. F. Lemanske Jr., C. A. Sorkness, M. Kraft, J. E. Fish, S. P. Peters, T. Craig, J. M. Drazen, J. G. Ford, E. Israel, R. J. Martin, E. A. Mauger, S. A. Nachman, J. D. Spahn, S. J. Szefler; Asthma Clinical Research Network of the National Heart, Lung, and Blood Institute, Long-acting β2-agonist monotherapy vs continued therapy with inhaled corticosteroids in patients with persistent asthma: A randomized controlled trial. *JAMA* **285**, 2583–2593 (2001).
3. T. Pera, R. B. Penn, Bronchoprotection and bronchorelaxation in asthma: New targets, and new ways to target the old ones. *Pharmacol. Ther.* **164**, 82–96 (2016).
4. E. Ricciotti, G. A. FitzGerald, Prostaglandins and inflammation. *Atertioscler. Thromb. Vasc. Biol.* **31**, 986–1000 (2011).
5. R. M. Breyer, C. K. Bagdassarian, S. A. Myers, M. D. Breyer, Prostanoid receptors: Subtypes and signaling. *Annu. Rev. Pharmacol. Toxicol.* **41**, 661–690 (2001).
6. S. J. Morgan, D. A. Deshpande, B. C. Tiegs, A. M. Misior, H. Yan, A. V. Hershfeld, T. C. Rich, R. A. Panettieri, S. S. An, R. B. Penn, β-Agonist-mediated relaxation of airway smooth muscle is protein kinase A-dependent. *J. Biol. Chem.* **289**, 23065–23074 (2014).
7. M. Zaccolo, Spatial control of cAMP signalling in health and disease. *Curr. Opin. Pharmacol.* **11**, 649–655 (2011).
8. V. P. Krymskaya, R. A. Panettieri Jr., Phosphodiesterases regulate airway smooth muscle function in health and disease. *Curr. Top. Dev. Biol.* **79**, 61–74 (2007).
9. C. K. Billington, O. O. Ojo, R. B. Penn, S. Ito, cAMP regulation of airway smooth muscle function. *Pulm. Pharmacol. Ther.* **26**, 112–120 (2013).
10. C. Mehats, S.-L. Jin, J. Wahlstrom, E. Law, D. T. Umetsu, M. Conti, PDE4D plays a critical role in the control of airway smooth muscle contraction. *FASEB J.* **17**, 1831–1841 (2003).
11. C. K. Billington, I. R. Le Jeune, K. W. Young, I. P. Hall, A major functional role for phosphodiesterase 4D5 in human airway smooth muscle cells. *Am. J. Respir. Cell Mol. Biol.* **38**, 1–7 (2008).
12. L. You, S. Feng, R. An, X. Wang, Osthole: A promising lead compound for drug discovery from a traditional Chinese medicine (TCM). *Nat. Prod. Commun.* **4**, 297–302 (2009).
13. Z.-R. Zhang, W. N. Leung, H. Y. Cheung, C. W. Chan, Osthole: A review on its bioactivities, pharmacological properties, and potential as alternative medicine. *Evid. Based Complement. Alternat. Med.* **2015**, 919616 (2015).
14. J. Wang, Y. Fu, Z. Wei, X. He, M. Shi, J. Kou, E. Zhou, W. Liu, Z. Yang, C. Guo, Anti-asthmatic activity of osthole in an ovalbumin-induced asthma murine model. *Respir. Physiol. Neurobiol.* **239**, 64–69 (2017).
15. C.-Y. Chiang, C.-C. Lee, C.-K. Fan, H.-M. Huang, B.-L. Chiang, Y.-L. Lee, Osthole treatment ameliorates Th2-mediated allergic asthma and exerts immunomodulatory effects on dendritic cell maturation and function. *Cell. Mol. Immunol.* **14**, 935–947 (2017).
16. N. K. Kordulewska, E. Kostyra, B. Chwala, M. Moszyńska, A. Cieślińska, E. Fiedorowicz, B. Jarmolowska, A novel concept of immunological and allergy interactions in autism spectrum disorders: Molecular, anti-inflammatory effect of osthole. *Int. Immunopharmacol.* **72**, 1–11 (2019).
17. Y. Huang, M. Sun, H. Cui, L. Kong, H. Zhai, Y. Wang, C. Lü, D. Fan, Vasorelaxant effect of osthole on isolated thoracic aortic rings in rats. *J. Tradit. Chin. Med.* **39**, 492–501 (2019).
18. F. N. Ko, T. S. Wu, M. J. Liou, T. F. Huang, C. M. Teng, Vasorelaxation of rat thoracic aorta caused by osthole isolated from *Angelica pubescens*. *Eur. J. Pharmacol.* **219**, 29–34 (1992).
19. C. M. Teng, C. H. Lin, F. N. Ko, T. S. Wu, T. F. Huang, The relaxant action of osthole isolated from *Angelica pubescens* in guinea-pig trachea. *Naunyn Schmiedebergs Arch. Pharmacol.* **349**, 202–208 (1994).
20. F. Fusi, G. Sgaragli, L. M. Ha, N. M. Cuong, S. Saponara, Mechanism of osthole inhibition of vascular Ca(v)1.2 current. *Eur. J. Pharmacol.* **680**, 22–27 (2012).
21. N.-N. Yang, H. Shi, G. Yu, C.-M. Wang, C. Zhu, Y. Yang, X.-L. Yuan, M. Tang, Z.-L. Wang, T. Gegen, Q. He, K. Tang, L. Lan, G. Y. Wu, Z.-X. Tang, Osthole inhibits histamine-dependent itch via modulating TRPV1 activity. *Sci. Rep.* **6**, 25657 (2016).
22. Y. Xie, H. Jiang, H. Nguyen, S. Jia, A. Berro, R. A. Panettieri Jr., D. W. Wolff, P. W. Abel, T. B. Casale, Y. Tu, Regulator of G protein signaling 2 is a key modulator of airway hyperresponsiveness. *J. Allergy Clin. Immunol.* **130**, 968–976.e3 (2012).
23. N. S. Holden, M. J. Bell, C. F. Rider, E. M. King, D. D. Gaunt, R. Leigh, M. Johnson, D. P. Siderovski, S. P. Heximer, M. A. Giembycz, R. Newton, β2-Adrenoceptor agonist-induced RGS2 expression is a genomic mechanism of bronchoprotection that is enhanced by glucocorticoids. *Proc. Natl. Acad. Sci. U.S.A.* **108**, 19713–19718 (2011).
24. S. J. Gunst, R. A. Panettieri Jr., Last Word on Point: Alterations in airway smooth muscle phenotype do cause airway hyperresponsiveness in asthma. *J. Appl. Physiol.* **113**, 847 (2012).
25. R. Léguillette, A.-M. Lauzon, Molecular mechanics of smooth muscle contractile proteins in airway hyperresponsiveness and asthma. *Proc. Am. Thorac. Soc.* **5**, 40–46 (2008).
26. M. Krause, E. W. Dent, J. E. Bear, J. J. Loureiro, F. B. Gertler, Ena/VASP proteins: Regulators of the actin cytoskeleton and cell migration. *Annu. Rev. Cell Dev. Biol.* **19**, 541–564 (2003).
27. R. Sood, G. Flint-Ashtamker, D. Borenstein, L. Barki-Harrington, Upregulation of prostaglandin receptor EP1 expression involves its association with cyclooxygenase-2. *PLOS ONE* **9**, e91018 (2014).
28. T. B. Johnstone, K. H. Smith, C. J. Koziol-White, F. Li, A. G. Kazarian, M. L. Corpuz, M. Shumyatcher, F. J. Ehlert, B. E. Himes, R. A. Panettieri Jr., R. S. Ostrom, PDE8 is expressed in human airway smooth muscle and selectively regulates cAMP signaling by β2-adrenergic receptors and adenylyl cyclase 6. *Am. J. Respir. Cell Mol. Biol.* **58**, 530–541 (2018).
29. A. G. Vang, S. Z. Ben-Sasson, H. Dong, B. Kream, M. P. DeNinno, W. Housley, R. B. Clark, P. M. Epstein, S. Brocke, PDE8 regulates rapid Teff cell adhesion and proliferation independent of ICER. *PLOS ONE* **5**, e12011 (2010).
30. O. Bruno, E. Fedele, J. Prickaerts, L. A. Parker, E. Canepa, C. Brullo, A. Cavallero, E. Gardella, A. Balbi, C. Domenicotti, E. Bollen, H. J. Gijselaers, T. Vanmierlo, K. Erb, C. L. Limebeer, F. Argellati, U. M. Marinari, M. A. Pronzato, R. Ricciarelli, GEBR-7b, a novel PDE4D selective

inhibitor that improves memory in rodents at non-emetic doses. *Br. J. Pharmacol.* **164**, 2054–2063 (2011).

31. G. B. Bolger, A. McCahill, E. Huston, Y. F. Cheung, T. McSorley, G. S. Baillie, M. D. Houslay, The unique amino-terminal region of the PDE4D5 cAMP phosphodiesterase isoform confers preferential interaction with β-arrestins. *J. Biol. Chem.* **278**, 49230–49238 (2003).

32. W. J. Rocque, G. Tian, J. S. Wiseman, W. D. Holmes, I. Zajac-Thompson, D. H. Willard, I. R. Patel, G. B. Wisely, W. C. Clay, S. H. Kadwell, C. R. Hoffman, M. A. Luther, Human recombinant phosphodiesterase 4B2B binds (R)-rolipram at a single site with two affinities. *Biochemistry* **36**, 14250–14261 (1997).

33. C. Zhang, Y. Xu, A. Chowdhary, D. Fox III, M. E. Gurney, H.-T. Zhang, B. D. Auerbach, R. J. Salvi, M. Yang, G. Li, J. M. O'Donnell, Memory enhancing effects of BPN14770, an allosteric inhibitor of phosphodiesterase-4D, in wild-type and humanized mice. *Neuropsychopharmacology* **43**, 2299–2309 (2018).

34. W. W. Busse, The relationship of airway hyperresponsiveness and airway inflammation: Airway hyperresponsiveness in asthma: Its measurement and clinical significance. *Chest* **138**, 4S–10S (2010).

35. T. Ozaki, S. I. Rennard, R. G. Crystal, Cyclooxygenase metabolites are compartmentalized in the human lower respiratory tract. *J. Appl. Physiol.* **62**, 219–222 (1987).

36. R. J. Gryglewski, Aspirin-induced asthma and cyclooxygenases, in *Selective COX-2 Inhibitors: Pharmacology, Clinical Effects and Therapeutic Potential*, J. Vane, J. Botting, Eds. (William Harvey Press and Kluwer Academic Publishers, 1998), pp. 99–107.

37. J. Buckley, M. A. Birrell, S. A. Maher, A. T. Nials, D. L. Clarke, M. G. Belvisi, EP$_4$ receptor as a new target for bronchodilator therapy. *Thorax* **66**, 1029–1035 (2011).

38. J. V. Michael, A. Gavrila, A. P. Nayak, T. Pera, J. R. Liberato, S. R. Polischak, S. D. Shah, D. A. Deshpande, R. B. Penn, Cooperativity of E-prostanoid receptor subtypes in regulating signaling and growth inhibition in human airway smooth muscle. *FASEB J.* **33**, 4780–4789 (2019).

39. F. Delamere, E. Holland, S. Patel, J. Bennett, I. Pavord, A. Knox, Production of PGE2 by bovine cultured airway smooth muscle cells and its inhibition by cyclo-oxygenase inhibitors. *Br. J. Pharmacol.* **111**, 983–988 (1994).

40. M. Profita, A. Sala, A. Bonanno, L. Riccobono, L. Siena, M. R. Melis, R. Di Giorgi, F. Mirabella, M. Gjomarkaj, G. Bonsignore, A. M. Vignola, Increased prostaglandin E2 concentrations and cyclooxygenase-2 expression in asthmatic subjects with sputum eosinophilia. *J. Allergy Clin. Immunol.* **112**, 709–716 (2003).

41. B. S. Patel, P. Prabhala, B. G. Oliver, A. J. Ammit, Inhibitors of phosphodiesterase 4, but not phosphodiesterase 3, increase β$_2$-agonist–induced expression of antiinflammatory mitogen-activated protein kinase phosphatase 1 in airway smooth muscle cells. *Am. J. Respir. Cell Mol. Biol.* **52**, 634–640 (2015).

42. Y.-F. Tsai, H.-P. Yu, P.-J. Chung, Y.-L. Leu, L.-M. Kuo, C.-Y. Chen, T.-L. Hwang, Osthol attenuates neutrophilic oxidative stress and hemorrhagic shock-induced lung injury via inhibition of phosphodiesterase 4. *Free Radic. Biol. Med.* **89**, 387–400 (2015).

43. C. Jørgensen, S. Yasmeen, H. K. Iversen, C. Kruuse, Phosphodiesterase4D (PDE4D)—A risk factor for atrial fibrillation and stroke? *J. Neurol. Sci.* **359**, 266–274 (2015).

44. R. X. Xu, A. M. Hassell, D. Vanderwall, M. H. Lambert, W. D. Holmes, M. A. Luther, W. J. Rocque, M. V. Milburn, Y. Zhao, H. Ke, R. T. Nolte, Atomic structure of PDE4: Insights into phosphodiesterase mechanism and specificity. *Science* **288**, 1822–1825 (2000).

45. K. Y. Zhang, G. L. Card, Y. Suzuki, D. R. Artis, D. Fong, S. Gillette, D. Hsieh, J. Neiman, B. L. West, C. Zhang, M. V. Milburn, S. H. Kim, J. Schlessinger, G. Bollag, A glutamine switch mechanism for nucleotide selectivity by phosphodiesterases. *Mol. Cell* **15**, 279–286 (2004).

46. A. B. Burgin, O. T. Magnusson, J. Singh, P. Witte, B. L. Staker, J. M. Bjornsson, M. Thorsteinsdottir, S. Hrafnsdottir, T. Hagen, A. S. Kiselyov, L. J. Stewart, M. E. Gurney, Design of phosphodiesterase 4D (PDE4D) allosteric modulators for enhancing cognition with improved safety. *Nat. Biotechnol.* **28**, 63–70 (2010).

47. H. Khairy, H. Saleh, A. M. Badr, M.-S. Marie, Therapeutic efficacy of osthole against dinitrobenzene sulphonic acid induced-colitis in rats. *Biomed. Pharmacother.* **100**, 42–51 (2018).

48. Y. Huang, Y. Xie, H. Jiang, P. W. Abel, R. A. Panettieri Jr., T. B. Casale, Y. Tu, Upregulated P-Rex1 exacerbates human airway smooth muscle hyperplasia in asthma. *J. Allergy Clin. Immunol.* **143**, 778–781.e5 (2019).

49. T. Raffay, P. Kc, J. Reynolds, P. Di Fiore, P. MacFarlane, R. J. Martin, Repeated β2-adrenergic receptor agonist therapy attenuates the response to rescue bronchodilation in a hyperoxic newborn mouse model. *Neonatology* **106**, 126–132 (2014).

50. C. Donovan, S. G. Royce, J. Esposito, J. Tran, Z. A. Ibrahim, M. L. Tang, S. Bailey, J. E. Bourke, Differential effects of allergen challenge on large and small airway reactivity in mice. *PLOS ONE* **8**, e74101 (2013).

51. Y. Xie, D. W. Wolff, M.-F. Lin, Y. Tu, Vasoactive intestinal peptide transactivates the androgen receptor through a protein kinase A-dependent extracellular signal-regulated kinase pathway in prostate cancer LNCaP cells. *Mol. Pharmacol.* **72**, 73–85 (2007).

52. Z. Otwinowski, W. Minor, Processing of x-ray diffraction data collected in oscillation mode. *Methods Enzymol.* **276**, 307–326 (1997).

53. E. Potterton, P. Briggs, M. Turkenburg, E. Dodson, A graphical user interface to the CCP4 program suite. *Acta Crystallogr. D Biol. Crystallogr.* **59**, 1131–1137 (2003).

54. P. D. Adams, P. V. Afonine, G. Bunkóczi, V. B. Chen, I. W. Davis, N. Echols, J. J. Headd, L.-W. Hung, G. J. Kapral, R. W. Grosse-Kunstleve, A. J. McCoy, N. W. Moriarty, R. Oeffner, R. J. Read, D. C. Richardson, J. S. Richardson, T. C. Terwilliger, P. H. Zwart, *PHENIX*: A comprehensive Python-based system for macromolecular structure solution. *Acta Crystallogr. D Biol. Crystallogr.* **66**, 213–221 (2010).

55. P. Emsley, K. Cowtan, *Coot*: model-building tools for molecular graphics. *Acta Crystallogr. D Biol. Crystallogr.* **60**, 2126–2132 (2004).

Science Signaling

Airway relaxation mechanisms and structural basis of osthole for improving lung function in asthma

Sheng Wang, Yan Xie, Yan-Wu Huo, Yan Li, Peter W. Abel, Haihong Jiang, Xiaohan Zou, Hai-Zhan Jiao, Xiaolin Kuang, Dennis W. Wolff, You-Guo Huang, Thomas B. Casale, Reynold A. Panettieri Jr., Taotao Wei, Zhengyu Cao and Yaping Tu

Breathing better with osthole

β_2-Adrenoreceptor agonists used to acutely relieve airway constriction in asthmatic patients become less effective with repeated use due to receptor desensitization and increase the risk of death. Using cells, lung slices, and mouse models of asthma, Wang *et al.* characterized osthole, a compound derived from a traditional Chinese medicine, in their search for compounds that induce bronchodilation through mechanisms other than activating β_2-adrenoreceptors. Osthole promoted airway relaxation by inhibiting the phosphodiesterase PDE4D to prevent the breakdown of the second messenger cAMP, resulting in amplification of prostaglandin E_2 signaling. These results suggest that variants of osthole could be developed to induce bronchodilation without desensitizing receptors or increasing the risk of death.

ARTICLE TOOLS	http://stke.sciencemag.org/content/13/659/eaax0273
RELATED CONTENT	http://stke.sciencemag.org/content/sigtrans/10/475/eaai8583.full http://stke.sciencemag.org/content/sigtrans/12/597/eaax3332.full http://immunology.sciencemag.org/content/immunology/5/48/eaba6087.full http://immunology.sciencemag.org/content/immunology/5/45/eaax8756.full
REFERENCES	This article cites 54 articles, 6 of which you can access for free http://stke.sciencemag.org/content/13/659/eaax0273#BIBL
PERMISSIONS	http://www.sciencemag.org/help/reprints-and-permissions

Use of this article is subject to the Terms of Service